Acta Geochim (2021) 40(1):13–24
https://doi.org/10.1007/s11631-020-00409-3

ORIGINAL ARTICLE

Niobium–tantalum oxide minerals in alluvial placer deposits from the Ngoura area, East-Cameroon

François Ndong Bidzang[1] · **Elisé Sababa**[2] · **Tessontsap Teutsong**[2]

Received: 15 October 2019 / Revised: 14 January 2020 / Accepted: 5 March 2020 / Published online: 13 March 2020

Abstract This work presents a preliminary mineralogical characterization of Nb–Ta oxide minerals from alluvial placers located in the Ngoura area, eastern Cameroon. The heavy minerals are characteristic of short hydromechanical transport and highlight the stability of Nb–Ta oxides during the weathering and transport. Nb–Ta mineralization in placer deposits from the Ngoura area may derive from local sedimentation. The assemblage of Nb–Ta oxides in the studied placers consists of tapiolite-(Fe) and tantalite-(Mn). Tapiolite-(Fe) exhibits high concentrations in Ta_2O_5 (78.07–80.46 wt%) and FeO (12.18–13.66 wt%) and plots within a narrow range of Ta* (0.900–0.933) and Mn* (0.037–0.119), which correspond to the ranges typically observed in tapiolite-(Fe) worldwide. Tantalite-(Mn) shows Ta_2O_5 contents ranging from 62.17 to 69.45 wt%, Nb_2O_5 from 12.09 to 17.37 wt%, MnO from 7.63 to 12.49 wt% and FeO from 1.48 to 6.62 wt%. It is also characterized by a wider range of Mn* (0.538–0.891) and relatively homogeneous Ta/(Ta + Nb) (0.683–0.779) ratios. Texturally, the studied Nb–Ta minerals exhibit oscillatory zoning characterized by bright Ta-rich zones alternating with dark Nb-rich zones. This oscillatory zoning is progressive in some minerals and the alternating bands may appear regular to wavy with gradual transitions. Oscillatory zoning in Nb–Ta oxides from the Ngoura placers is considered to be a primary magmatic feature and is tentatively explained as a result of magmas mixing, rapid cooling or degassing/decompression of the igneous system. The geomorphology and the tropical humid climate of the eastern region offer suitable conditions for the deposition of alluvial placers. Therefore, niobium-tantalum minerals from the Ngoura placers must have been sourced from the weathering and erosion of alkaline granites and pegmatites widespread in the study area.

Keywords Niobium · Tantalum · Tapiolite-(Fe) · Tantalite-(Mn) · Ngoura placer · East Cameroon

✉ François Ndong Bidzang
fndongbidzang@gmail.com

[1] Ore Processing Laboratory, Institute of Geological and Mining Research, P.O. Box 4110, Yaoundé, Cameroon

[2] Department of Earth Sciences, University of Yaoundé 1, P.O. Box 812, Yaoundé, Cameroon

1 Introduction

Niobium (Nb) and tantalum (Ta) are transition metals in group 5 of the periodic table and have nearly similar chemical and physical properties (Nowak and Ziolek 1999). Niobium is a soft and ductile metal with a variety of uses such as niobium carbide, steel alloys and conducting magnets (Mitchell 2015). The world's mining production of Nb ores comes from carbonatites and their weathered-enriched materials (Mackay and Simandl 2014). Tantalum is a hard but ductile metal, extensively used for electronic applications, superalloys, specialty metal products for medical and chemical industries (Melcher et al. 2015). It is recovered from oxide minerals that are present in pegmatites, peraluminous granites, as well as their weathered equivalents and placers (Mackay and Simandl 2014; Simandl et al. 2018). The main ore minerals of Ta and Nb include pyrochlore group, columbite-tantalite group, tapiolite group, wodginite group, perovskite, ixiolite, and euxenite groups (Mackay and Simandl 2015). Major Nb and Ta deposits are dated 2.8 Ga–85 Ma (Mackay and Simandl 2014).

Cameroon hosts several mineral occurrences such as iron ore (e.g., Ndong et al. 2016; Teutsong et al. 2017; Ganno et al. 2018; Soh Tamehe et al. 2019), bauxite ore (Nguimatsa et al. 2019a), gemstones (Kanouo et al. 2016; Mbih et al. 2016), alluvial rutile (Tonje et al. 2014; Mbanga Nyobe et al. 2018) and gold (Vishiti et al. 2015; Ndong et al. 2015; Nguimatsa et al. 2019b). The eastern part of the country is known for extensively on-going artisanal mining of alluvial gold/diamond deposits. Columbo-tantalite (coltan) occurrences have been historically identified in Mayo Darlé (Adamawa Region, North Cameroon) and Garga-Sarali (East Cameroon) (Ntep Gweth et al. 2003). Fosso Tchunte et al. (2018) recently investigated Nb–Ta oxides in leucogranites from the Mayo Salah region (Northern Cameroon). Despite extensive exploration campaigns conducted in Cameroon, there is a lack of scientific data on these highly demanded metals. This paper is focused on the mineralogical and chemical investigation of Nb–Ta oxides occurring in alluvial placer deposits from the Ngoura area in eastern Cameroon, with the aim of constraining their possible sources and genesis.

2 Geological setting

Ngoura belongs to the Central African Fold Belt (CAFB) in Cameroon, which is defined as a major collisional belt that underlies the region from the West African Craton to East Africa (Van Schmus et al. 2008). The CAFB is Neoproterozoic in age, bounded to the south by the Congo craton and to the west by the West African craton. It has been subdivided into three lithostructural units which are from the south to the north: the Yaoundé domain, the Adamawa-Yadé domain, and the Northwestern Cameroon domain (Toteu et al. 2004; Van Schmus et al. 2008).

The study area is situated within the Adamawa-Yadé lithostructural unit which represents a Paleoproterozoic basement that was dismembered during the Pan-African orogeny. It is dominated by 640–610 Ma syn- to late-collisional high-K calc-alkaline granitoids, which intrude high-grade gneisses (Toteu et al. 2004; Njiosseu et al. 2005; Van Schmus et al. 2008; Asaah et al. 2015). This domain is dissected by large NE-striking transcurrent faults thought to be extensions of the major shear zones of north-eastern Brazil. Toteu et al. (2004) identified three main groups in the Adamawa-Yadé domain: (i) large remnants of Paleoproterozoic metasediments and orthogneisses with contributions from an Archaean crust similar to the Ntem Complex; (ii) low- to medium-grade metasedimentary and acidic volcanoclastic rocks; (iii) and syn- to late-tectonic granitoids mainly of transitional composition of crustal origin.

At the local scale, the study area belongs to the Boden gold district (Fig. 1). It is underlain by a large complex of late- to post-tectonic calc-alkaline to alkaline granite plutons (Suh et al. 2006). The early granite plutons are low-grade metamorphosed, variably deformed and foliated at their margins. Generally, the granites contain xenoliths and inliers of the older schists, pre- to syn-tectonic granites and gneissic basement. Some granite plutons appear sheared and cross-cut by NE–SW trending pegmatitic and quartz veins (Suh et al. 2006). Tourmaline alteration is commonly observed in the wall rock. Recent geological investigations in the Ngoura area have recognized orthogneisses and migmatites intruded by syn- to post-tectonic granites and granodiorites (Takodjou Wambo et al. 2016, 2018).

3 Methodology

Stream sediment samples used in this study were collected at various points within the drainage basin (Fig. 2) defining an area of $\sim$ 735 km^2. A total of 42 samples were collected at suitable sites of the Koubou and Oudou rivers tributaries. All sampling sites were located using a GPS and coordinates recorded into a GIS platform. During the sampling process, the thickness of the sterile overburden and the gravel was measured. To eliminate larger clasts in gravels collected from the dug pits, samples were sieved with a filter of mesh size 10 mm. All the smaller size grains which passed through the sieve were collected and washed. Samples were placed in a pan and shaken sideways in a circular motion while being held just under the water. Heavy minerals sink to the bottom and light minerals rise and spill out over the top. The analytical procedures are similar to those described previously by McClenaghan et al. (2011). The heavy mineral fraction was retained and placed in a plastic bag together with the sample tag before the bag was stapled shut. At the base camp, the heavy mineral fraction was dried and the Nb–Ta oxide grains were handpicked under a binocular microscope (Fig. 3).

Niobium-tantalum oxide grains were selected for microanalyses at the laboratory of microanalyses (LMA) of the University of Laval, Canada. Zoning and mineral chemistry of Nb–Ta minerals were performed using wavelength-dispersive spectrometry (WDS) with a Cameca SX-100 electron microprobe. The microprobe was operated at 15 kV and 20 nA, and an electron beam diameter of 5 μm. Counting time for Fe, Mn, Nb, Ta, Ti, and Sc was 10 s, for W 90 s, for Sn and Zr 100 s and for Hf 120 s. The following natural mineral and metal standards were used: columbite (Nb Lα), tapiolite (Ta Lα), magnetite (Fe Kα), rhodonite (Mn Kα), scandium (Sc Kα), rutile (Ti Kα), hafnium (Hf Lα), zirconium (Zr Lα), tin (Sn Lα), tungsten (W Lα), and uranium (U Mα). The detection limit for most

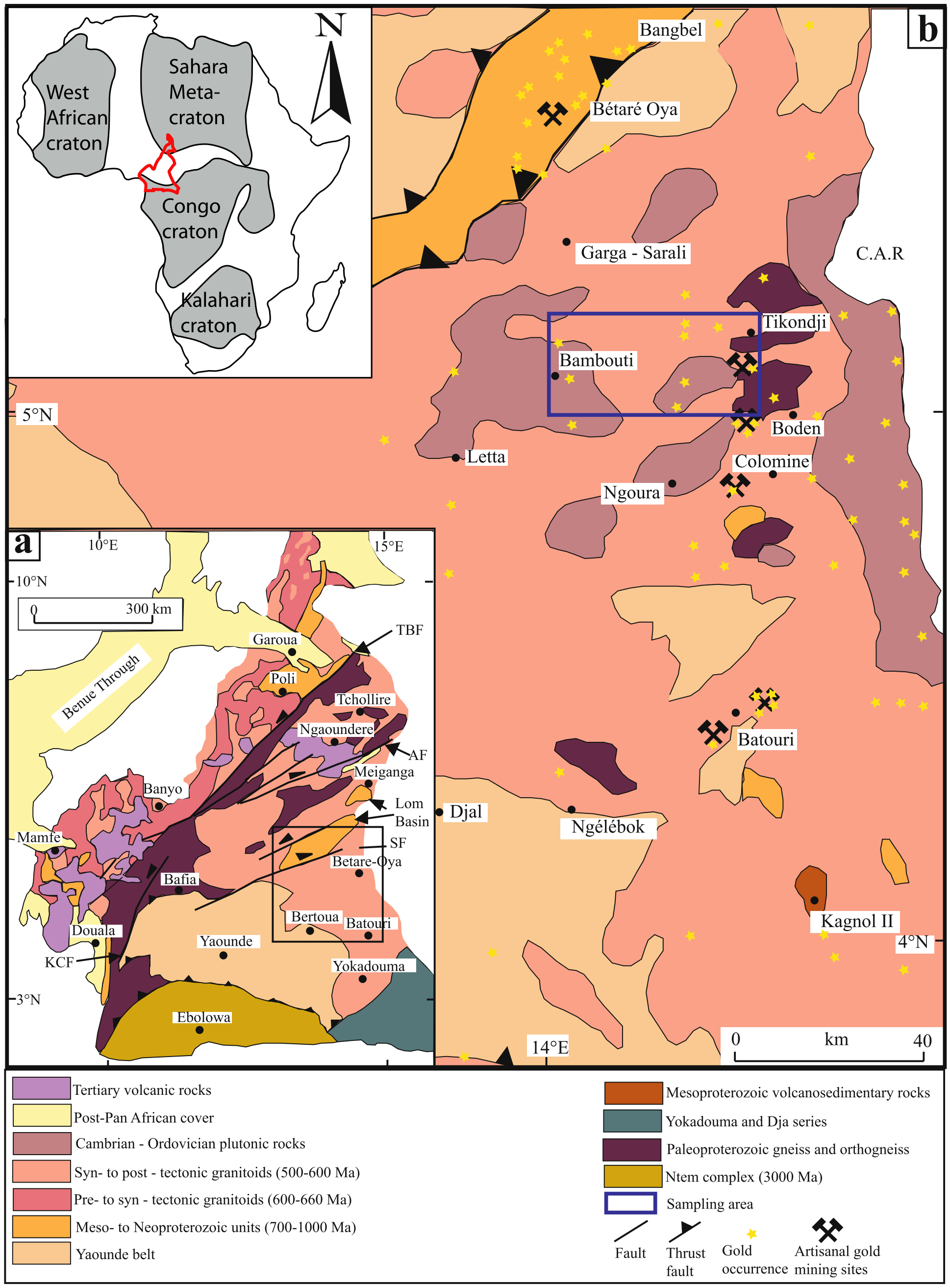

Fig. 1 Geology of South-East Cameroon (Asaah et al. 2015). **a** Geological map of Cameroon. The Central African Shear Zone is defined by a system of NE-trending faults comprising Tchollire-Banyo Fault (TBF), Adamawa Fault (AF), Sanaga Fault (SF) and Kribi-Campo Fault (KCF). **b** Regional geological map of southeastern Cameroon, showing artisanal gold mining sites and other reported gold occurrences

elements is 200 ppm. The mineral formulae of Nb–Ta minerals were calculated based on six atoms of oxygen per formula unit (Tables 1 and 2).

4 Results

4.1 Morphological features

The depths of the pits are variable from 2 to 4 m with the bedrock comprising of granitoids (Fig. 3a). The sterile which is made up of silt and clay has a thickness between 1 and 1.5 m and the gravel located at the bottom of the pit is the mineralized zone. The latter is composed of pebble, sand, silt, and clay. Sample separation and heavy mineral extraction show that the concentrates are mostly composed of quartz and Nb–Ta oxides when observed with the naked eye. The heavy mineral fraction displays well-formed crystals with crystalline growth faces, straight borders and rounded edges (Fig. 3d).

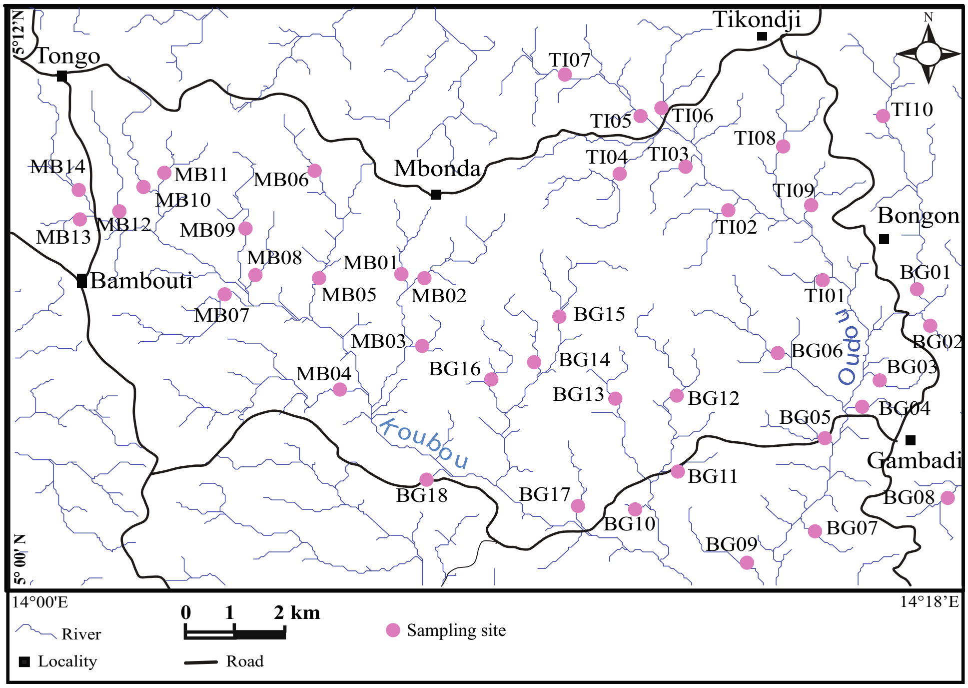

Fig. 2 Drainage pattern map showing sampling sites

4.2 Mineral chemistry

Electron microprobe data of Nb–Ta minerals from the Ngoura placers are given in Tables 1 and 2. A total of 42 analyses have been carried out on the core of each crystal, corresponding to columbite group minerals (CGM) and tapiolite group minerals. Atomic compositions and ratios were calculated and plotted on the columbite quadrilateral, where two distinct groups of Nb–Ta oxides were identified: tantalite-(Mn) and tapiolite-(Fe) (Fig. 4).

Tantalite-(Mn) is characterized by Ta_2O_5 contents ranging from 62.17 to 69.45 wt%, Nb_2O_5 from 12.09 to 17.37 wt%, MnO from 7.63 to 12.49 wt% and FeO from 1.48 to 6.62 wt% (Table 1). Minor elements vary from 0.12 to 0.64 wt% TiO_2 and 0.01 to 0.37 wt% SnO_2. Na, U, Th, and the analyzed REE (La, Ce, Nd) display very low contents. Tantalite-(Mn) from the Ngoura placers is relatively homogeneous in Ta/(Ta + Nb) (0.683–0.779) but it shows wide variations in Mn/(Mn + Fe) ratios (0.538–0.891) (Table 1). According to their Mn/(Mn + Fe) ratios, tantalite-(Mn) crystals can be divided into two groups (Fig. 4). Group 1 shows Mn/(Mn + Fe) < 0.60 and is distributed on the eastern drainage network while group 2 is characterized by higher Mn/(Mn + Fe) ratios (> 0.60) and occurs in the center and western parts of the study area (Fig. 5).

Tapiolite-(Fe) from the Ngoura area exhibits higher and rather constant concentrations in Ta_2O_5 (78.07–80.46 wt%) and FeO (12.18–13.66 wt%). Slightly variable contents were obtained for Nb_2O_5 and MnO, ranging 3.49–5.21 wt% and 0.52–1.64 wt%, respectively (Table 2). Minor oxides display comparable ranges, namely 0.19–0.61 wt% TiO_2 and 0.13–0.65 wt% SnO_2. Tapiolite-(Fe) compositions show typically very low and variable Mn/(Mn + Fe) but very high and nearly constant Ta/(Ta + Nb) atomic ratios: 0.037–0.119 and 0.900–0.933, respectively (Table 2). Tapiolite-(Fe) samples are distributed throughout the study area (Fig. 5).

4.3 Textural features

Backscattered electron images illustrate typical zoning patterns of Nb–Ta oxide minerals from the Ngoura placers (Fig. 6). Lahti (1987) described three types of zoning in CGM: progressive, oscillatory and patchy-replacement, using columbite-tantalite crystals from the granitic pegmatites in southern Finland. Oscillatory zoning is the most common feature found in the studied Nb–Ta minerals. It is characterized by bright Ta-rich zones alternating with dark Nb-rich zones (Fig. 6a). This oscillatory zoning is usually progressive (Fig. 6b), evolving from Nb-rich cores to Ta-rich rims. The episodic zones form thin to medium and well-defined layers from the core to rim, commonly regular and more rarely curved or wavy (Fig. 6a). In other cases, alternating zones appear as coarse bands with gradual transitions, truncated in the border zone (Fig. 6c).

Fig. 3 Overview of the Ngoura alluvial placer and sample collection. **a** Field photograph of artisanal mining site. **b** Typical profile of alluvial Nb–Ta deposit in the study area. **c** Mineralized gravel collected from alluvial profile. **d** Nb–Ta oxide minerals collected from mineralized gravel

5 Discussion

5.1 Chemical features

The assemblage of analyzed Nb–Ta minerals from the Ngoura placers consists of tapiolite-(Fe) and tantalite-(Mn). Tapiolite-(Fe) plots within a narrow range of Ta* (0.900–0.933) and Mn* (0.037–0.119) values (see Fig. 4), which correspond to the ranges typically observed in Tapiolite-(Fe) (Černý et al. 1992; Wise and Černý 1996). Tantalite-(Mn) displays a wider range of Mn* (0.538–0.891), suggesting variable source rocks. Nb–Ta oxide minerals from the Ngoura deposit display higher concentrations in tantalum compared to those of most of African Ta provinces (Melcher et al. 2015). Fluorinity is commonly used to decipher fractionation behavior of CGM in pegmatites (Černý 1992; Alfonso et al. 1995). Tapiolite-(Fe) is usually found in the F-poor system whereas tantalite-(Mn) occurs in more evolved F-rich environments (Tindle and Breaks 2000). When comparing with the studied Nb–Ta minerals, Nb–Ta oxides from the Mayo Salah leucogranite exclusively consist of columbite-Mn (Fosso Tchunte et al. 2018).

5.2 Zoning patterns

Nb–Ta oxides from the Ngoura placers exhibit oscillatory zoning which appears to be progressive in places. These features were also observed in CGM (columbite-Mn) from the Mayo Salah leucogranite (Fosso Tchunte et al. 2018). Oscillatory zoning is certainly the most observed type of zoning in CGM and many examples are reported in the literature (e.g., Lahti 1987; Alfonso et al. 1995; Van Lichtervelde et al. 2007). Zoning in CGM is commonly considered to be a primary magmatic feature (Tindle and Breaks 2000). In progressive zoning, crystals show smooth

Table 1 Electron microprobe analyses (wt%) of tantalite-(Mn) from the Ngoura placer

Sample	TI02	TI04	TI05	TI07	TI08	TI10	BG01	BG03	BG05	BG06	BG07	BG08	BG09	BG10	BG14	BG18
MnO	10.48	7.79	7.63	7.64	8.13	8.17	7.84	7.78	7.71	7.83	7.67	7.64	8.18	12.23	11.00	10.03
FeO	3.48	6.46	6.47	6.53	5.96	5.79	6.20	6.28	6.62	6.40	6.59	6.53	5.96	2.01	3.05	4.18
Nb_2O_5	14.10	13.06	12.53	12.65	12.40	12.38	12.23	12.33	13.06	13.08	13.22	12.65	12.36	17.37	16.00	15.42
Ta_2O_5	67.02	67.51	68.43	68.38	68.72	68.65	68.88	68.96	67.78	68.00	67.59	68.38	68.43	62.17	63.86	64.68
SnO_2	0.05	0.06	0.26	0.12	0.10	0.10	0.37	0.04	0.07	0.06	0.22	0.12	0.11	0.03	0.05	0.07
U_2O_3	0.08	0.09	0.09	0.07	0.08	0.08	0.08	0.09	0.08	0.07	0.07	0.07	0.09	0.10	0.11	0.09
Na_2O	0.03	0.02	0.02	0.03	0.03	0.02	0.03	0.03	0.03	0.03	0.02	0.03	0.02	0.03	0.02	0.03
Nd_2O_3	0.12	0.15	0.14	0.15	0.11	0.11	0.14	0.16	0.11	0.17	0.15	0.15	0.17	0.12	0.11	0.16
TiO_2	0.33	0.64	0.29	0.37	0.34	0.33	0.43	0.42	0.52	0.51	0.36	0.37	0.33	0.35	0.55	0.41
ThO_2	0.02	0.05	0.04	0.05	0.02	0.05	0.04	0.04	0.02	0.02	0.02	0.05	0.03	0.05	0.05	0.04
Ce_2O_3	0.06	0.06	0.05	0.05	0.05	0.08	0.05	0.05	0.05	0.05	0.05	0.05	0.09	0.09	0.06	0.06
La_2O_3	0.00	0.00	0.00	0.00	0.00	0.00	0.01	0.00	0.03	0.00	0.01	0.00	0.00	0.00	0.01	0.00
Total	95.78	95.87	95.95	96.01	95.93	95.73	96.28	96.16	96.06	96.22	95.95	96.01	95.76	94.54	94.86	95.16
Formulae calculated to 6 atoms of O																
Mn	0.719	0.531	0.520	0.520	0.555	0.559	0.535	0.531	0.525	0.533	0.522	0.520	0.559	0.832	0.751	0.683
Fe	0.237	0.444	0.452	0.454	0.416	0.406	0.431	0.436	0.455	0.439	0.456	0.454	0.418	0.135	0.206	0.287
Nb	0.515	0.477	0.458	0.462	0.453	0.453	0.446	0.450	0.477	0.477	0.483	0.462	0.452	0.631	0.583	0.561
Ta	1.480	1.495	1.530	1.523	1.536	1.539	1.535	1.536	1.500	1.502	1.500	1.523	1.533	1.359	1.401	1.424
Sn	0.002	0.002	0.010	0.004	0.004	0.004	0.014	0.001	0.003	0.002	0.008	0.004	0.004	0.001	0.002	0.002
U	0.001	0.002	0.002	0.001	0.002	0.002	0.002	0.002	0.002	0.001	0.001	0.001	0.002	0.002	0.002	0.002
Na	0.004	0.004	0.004	0.004	0.004	0.003	0.004	0.004	0.004	0.004	0.004	0.004	0.004	0.006	0.003	0.005
Nd	0.003	0.004	0.004	0.004	0.003	0.003	0.004	0.005	0.003	0.005	0.004	0.004	0.005	0.003	0.003	0.004
Ti	0.020	0.039	0.018	0.022	0.021	0.020	0.026	0.026	0.032	0.031	0.022	0.022	0.020	0.021	0.034	0.025
Th	0.000	0.001	0.001	0.001	0.000	0.001	0.001	0.001	0.000	0.000	0.000	0.001	0.000	0.001	0.001	0.001
Ce	0.002	0.002	0.001	0.001	0.001	0.002	0.001	0.001	0.001	0.001	0.001	0.001	0.003	0.003	0.002	0.002
La	0.000	0.000	0.000	0.000	0.000	0.000	0.000	0.000	0.001	0.000	0.000	0.000	0.000	0.000	0.000	0.000
Total	2.985	3.001	2.999	2.998	2.995	2.991	3.000	2.993	3.002	2.998	3.002	2.998	3.000	2.993	2.988	2.995
Ta/Nb	2.874	3.134	3.341	3.297	3.391	3.397	3.442	3.413	3.145	3.149	3.106	3.297	3.392	2.154	2.403	2.538
Mn/Mn + Fe	0.752	0.545	0.535	0.534	0.572	0.579	0.554	0.549	0.536	0.548	0.534	0.534	0.572	0.860	0.785	0.704
Ta/Ta + Nb	0.742	0.758	0.770	0.767	0.772	0.773	0.775	0.773	0.759	0.759	0.756	0.767	0.772	0.683	0.706	0.717

Table 1 continued

Sample	MB01	MB02	MB03	MB04	MB05	MB06	MB09	MB10	MB12	MB13	MB14	Average
MnO	10.22	9.84	9.79	12.49	9.71	9.83	9.79	9.67	9.63	9.64	8.27	9.13
FeO	4.01	4.19	4.27	1.48	4.61	4.40	4.45	4.59	4.46	4.53	5.80	5.01
Nb_2O_5	16.23	13.38	13.47	15.25	14.21	14.23	14.20	14.36	13.68	13.79	12.09	13.69
Ta_2O_5	63.48	67.56	67.65	65.70	66.46	66.68	66.20	66.27	67.12	67.06	69.45	67.08
SnO_2	0.05	0.34	0.01	0.03	0.04	0.04	0.03	0.19	0.24	0.09	0.08	0.11
U_2O_3	0.11	0.07	0.07	0.06	0.07	0.05	0.07	0.05	0.07	0.05	0.06	0.08
Na_2O	0.03	0.03	0.03	0.03	0.03	0.03	0.03	0.03	0.03	0.03	0.03	0.03
Nd_2O_3	0.20	0.06	0.08	0.04	0.03	0.09	0.07	0.07	0.06	0.07	0.09	0.11
TiO_2	0.52	0.26	0.25	0.16	0.35	0.34	0.47	0.19	0.12	0.20	0.25	0.36
ThO_2	0.02	0.06	0.06	0.05	0.05	0.05	0.07	0.05	0.07	0.07	0.05	0.04
Ce_2O_3	0.05	0.09	0.09	0.11	0.09	0.10	0.10	0.09	0.09	0.09	0.08	0.07
La_2O_3	0.00	0.01	0.00	0.00	0.03	0.00	0.00	0.01	0.00	0.00	0.00	0.00
Total	94.92	95.89	95.78	95.39	95.68	95.83	95.48	95.57	95.56	95.63	96.25	95.71
Formulae calculated to 6 atoms of O												
Mn	0.696	0.670	0.666	0.854	0.661	0.669	0.666	0.658	0.655	0.656	0.563	0.623
Fe	0.271	0.296	0.301	0.102	0.319	0.303	0.309	0.320	0.317	0.319	0.407	0.348
Nb	0.590	0.487	0.490	0.556	0.517	0.517	0.517	0.523	0.498	0.502	0.441	0.499
Ta	1.390	1.504	1.505	1.448	1.468	1.471	1.464	1.468	1.498	1.491	1.552	1.488
Sn	0.002	0.013	0.000	0.001	0.002	0.001	0.001	0.007	0.009	0.003	0.003	0.004
U	0.002	0.002	0.002	0.001	0.002	0.001	0.002	0.001	0.002	0.001	0.001	0.002
Na	0.004	0.006	0.006	0.006	0.006	0.006	0.005	0.005	0.005	0.006	0.005	0.005
Nd	0.006	0.002	0.002	0.001	0.001	0.003	0.002	0.002	0.002	0.002	0.003	0.003
Ti	0.032	0.016	0.016	0.010	0.021	0.021	0.029	0.012	0.007	0.012	0.016	0.022
Th	0.000	0.001	0.001	0.001	0.001	0.001	0.001	0.001	0.001	0.001	0.001	0.001
Ce	0.001	0.003	0.003	0.003	0.003	0.003	0.003	0.003	0.003	0.003	0.002	0.002
La	0.000	0.000	0.000	0.000	0.001	0.000	0.000	0.000	0.000	0.000	0.000	0.000
Total	2.995	2.998	2.991	2.983	3.000	2.996	2.999	3.000	2.997	2.996	2.994	2.996
Ta/Nb	2.356	3.088	3.071	2.604	2.839	2.845	2.832	2.807	3.008	2.970	3.519	3.015
Mn/Mn + Fe	0.720	0.694	0.689	0.893	0.674	0.688	0.683	0.673	0.674	0.673	0.580	0.642
Ta/Ta + Nb	0.702	0.755	0.754	0.723	0.740	0.740	0.739	0.737	0.751	0.748	0.779	0.749

Table 2 Electron microprobe analyses (wt%) of tapiolite-(Fe) from the Ngoura placer

Sample	TI01	TI03	TI06	TI09	BG02	BG04	BG11	BG12	BG13	BG15	BG16	BG17	MB07	MB08	MB11	Average
MnO	1.14	0.75	0.84	1.14	1.06	1.13	0.72	1.21	1.23	0.55	0.52	0.72	1.02	1.64	1.09	0.98
FeO	12.61	13.18	13.05	12.68	12.85	12.81	13.53	12.66	13.01	13.66	13.60	13.53	13.09	12.18	12.87	13.02
Nb_2O_5	3.57	4.32	4.24	3.62	4.37	4.42	5.19	4.17	4.88	5.21	4.64	5.19	4.51	3.49	4.39	4.41
Ta_2O_5	80.38	79.26	79.66	80.17	79.21	79.50	78.51	79.74	78.07	78.15	78.94	78.51	79.23	80.46	79.02	79.25
SnO_2	0.65	0.28	0.61	0.33	0.35	0.34	0.17	0.13	0.15	0.47	0.37	0.17	0.20	0.16	0.34	0.31
U_2O_3	0.04	0.05	0.03	0.05	0.04	0.03	0.01	0.04	0.05	0.03	0.03	0.01	0.02	0.04	0.05	0.03
Na_2O	0.02	0.01	0.02	0.01	0.01	0.02	0.02	0.01	0.01	0.01	0.02	0.02	0.02	0.02	0.01	0.02
Nd_2O_3	0.07	0.13	0.14	0.15	0.03	0.10	0.11	0.06	0.11	0.07	0.07	0.11	0.04	0.12	0.08	0.09
TiO_2	0.19	0.48	0.36	0.17	0.26	0.27	0.52	0.39	0.61	0.29	0.30	0.52	0.35	0.22	0.40	0.36
ThO_2	0.04	0.06	0.04	0.04	0.05	0.02	0.02	0.04	0.03	0.02	0.04	0.02	0.02	0.02	0.04	0.03
Ce_2O_3	0.00	0.01	0.00	0.05	0.03	0.00	0.00	0.03	0.06	0.00	0.00	0.00	0.00	0.05	0.01	0.02
La_2O_3	0.01	0.00	0.01	0.00	0.03	0.00	0.03	0.03	0.03	0.04	0.03	0.03	0.03	0.00	0.00	0.02
Total	98.69	98.52	98.98	98.41	98.28	98.63	98.83	98.50	98.23	98.50	98.56	98.83	98.55	98.39	98.28	98.55
Formulae calculated to 6 atoms of O																
Mn	0.082	0.053	0.060	0.082	0.076	0.080	0.051	0.087	0.088	0.039	0.037	0.051	0.073	0.117	0.078	0.070
Fe	0.893	0.926	0.916	0.900	0.906	0.901	0.941	0.890	0.911	0.956	0.955	0.941	0.919	0.864	0.906	0.915
Nb	0.137	0.164	0.160	0.139	0.166	0.167	0.195	0.158	0.184	0.197	0.176	0.195	0.171	0.134	0.167	0.167
Ta	1.852	1.812	1.818	1.850	1.819	1.819	1.776	1.826	1.779	1.780	1.803	1.776	1.809	1.856	1.812	1.812
Sn	0.024	0.010	0.023	0.012	0.013	0.013	0.006	0.005	0.006	0.018	0.014	0.006	0.008	0.006	0.013	0.012
U	0.001	0.001	0.001	0.001	0.001	0.001	0.000	0.001	0.001	0.001	0.001	0.000	0.001	0.001	0.001	0.001
Na	0.002	0.002	0.002	0.002	0.001	0.002	0.003	0.002	0.002	0.002	0.002	0.003	0.003	0.002	0.002	0.002
Nd	0.002	0.004	0.004	0.005	0.001	0.003	0.003	0.002	0.003	0.002	0.002	0.003	0.001	0.004	0.002	0.003
Ti	0.012	0.030	0.022	0.011	0.016	0.017	0.032	0.025	0.038	0.018	0.019	0.032	0.022	0.014	0.025	0.022
Th	0.001	0.001	0.001	0.001	0.001	0.000	0.000	0.001	0.000	0.000	0.001	0.000	0.000	0.000	0.001	0.001
Ce	0.000	0.000	0.000	0.001	0.001	0.000	0.000	0.001	0.002	0.000	0.000	0.000	0.000	0.001	0.000	0.000
La	0.000	0.000	0.000	0.000	0.001	0.000	0.001	0.001	0.001	0.001	0.001	0.001	0.001	0.000	0.000	0.001
Total	3.006	3.004	3.008	3.003	3.003	3.004	3.010	2.997	3.014	3.015	3.011	3.010	3.008	3.000	3.007	3.007
Ta/Nb	13.518	11.049	11.363	13.309	10.958	10.892	9.108	11.557	9.668	9.036	10.244	9.108	10.579	13.851	10.850	11.006
Mn/Mn + Fe	0.084	0.054	0.061	0.084	0.077	0.082	0.051	0.089	0.088	0.039	0.037	0.051	0.074	0.119	0.079	0.071
Ta/Ta + Nb	0.931	0.917	0.919	0.930	0.916	0.916	0.901	0.920	0.906	0.900	0.911	0.901	0.914	0.933	0.916	0.915

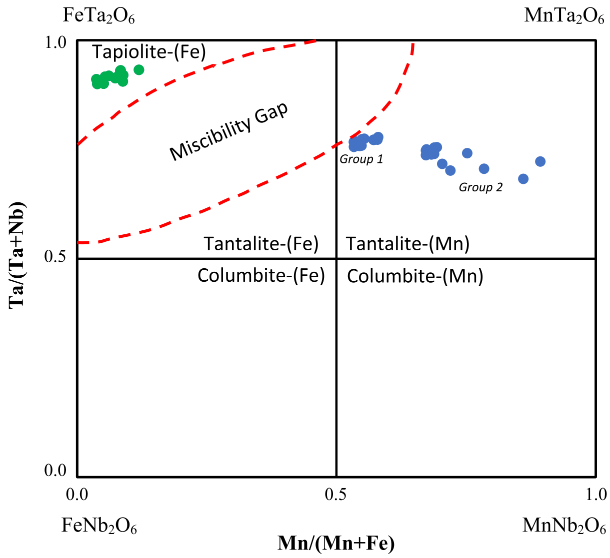

Fig. 4 Compositions of tapiolite-(Fe) and tantalite-(Mn) plotted in the columbite quadrilateral diagram

compositional variation between the rim and core. In oscillatory zoned crystals, the composition varies periodically between the core and the rim (Lahti 1987). The origin of oscillatory zoning has been explained in different ways by several authors and remains controversial. In igneous systems, this zoning is commonly related to magma mixing, rapid cooling or degassing/decompression of the system (Holten et al. 1997; Badanina et al. 2015; Llorens González et al. 2017).

5.3 Comparative mineralogy

Tantalum-Niobium minerals in Africa are commonly associated with granites and pegmatites. They are mostly recovered from weathered pegmatites or from eluvial and alluvial placer deposits (Melcher et al. 2015). The mineralogy of the studied Ta–Nb oxides revealed oscillatory zoned tapiolite-(Fe) and tantalite-(Mn) grains whilst Ta–Nb minerals in placer from the Kokobin deposit (Ghana) consists of complexly zoned and partly homogeneous columbite-(Mn) to tantalite-(Mn) minerals (Melcher et al. 2015). When compared to the Ngoura deposit, placers investigated in the Archean–Paleoproterozoic transition zone at the southern margin of the Congo Craton displays a different mineral assemblage, including complexly zoned columbite-(Fe) to tantalite-(Fe), tapiolite, and subordinate U-bearing microlite (Melcher et al. 2015). Similarly, the mineralogy of heavy mineral concentrates from the Jos Plateau placer deposit in Nigeria is completely different to that of the Ngoura deposit, and characterized by columbite-(Fe), tantalite-(Fe) and columbite-(Mn), tapiolite, ixiolite, microlite, fergusonite, euxenite and cassiterite (Mücke and Neumann 2006).

5.4 Genesis of Ta–Nb mineralization

Large Ta–Nb deposits are mined from granites, pegmatites, and carbonatites. Placer deposits have historically provided up to 40% of world Ta production (Mackay and Simandl

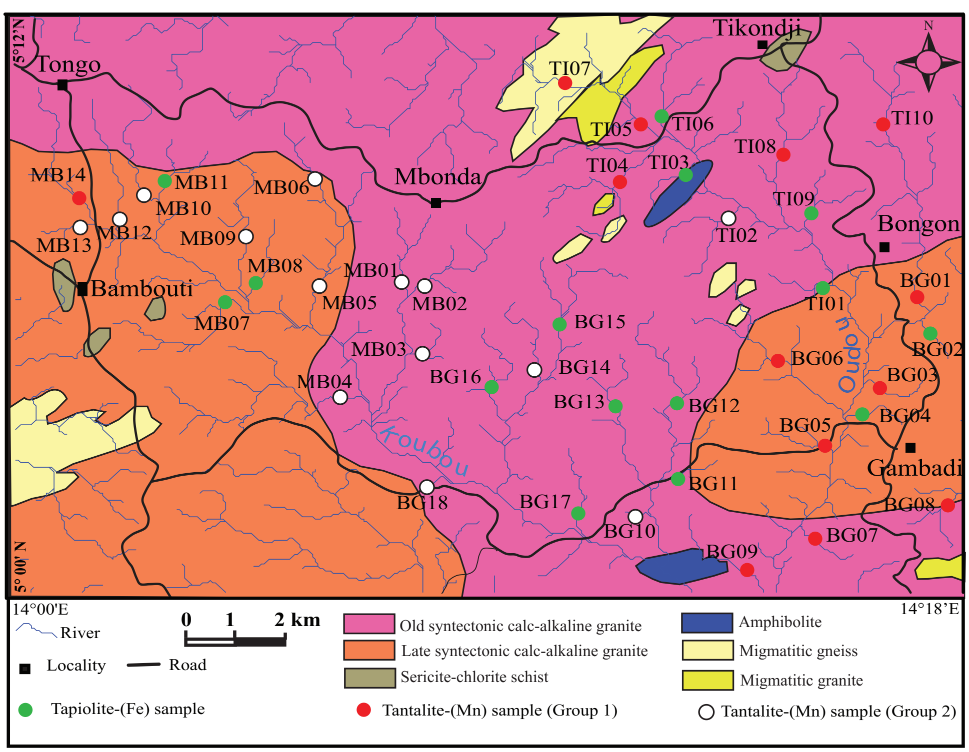

Fig. 5 Local geology and drainage pattern map showing tapiolite-(Fe) and tantalite-(Mn) distribution throughout the study area

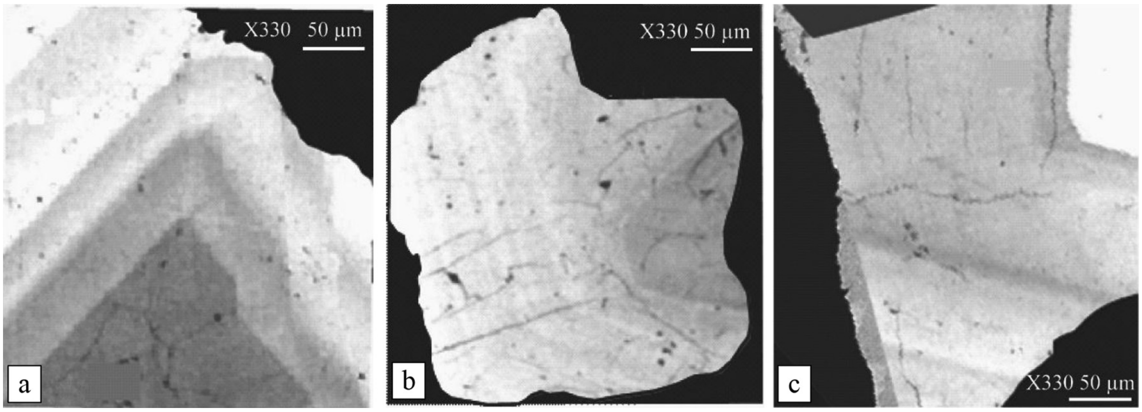

Fig. 6 Backscattered electron images of Nb–Ta minerals from Ngoura. **a** Oscillatory zoning; **b** progressive oscillatory zoning; **c** irregular oscillatory zoning truncated in the border zone

2014). In the eastern part of Cameroon, there are abundant alkaline granites and pegmatitic rocks that have never been investigated for Ta–Nb mineralization. The mineral assemblage of the Ngoura sediments is characteristic of hydromechanical transport. The high proportion of Nb–Ta oxides in the alluvia may be linked to their stability during the weathering process and in the alluvial environment. The grain size of quartz and Nb–Ta oxides extremely depends on the textural features of their source rocks (Bassis et al. 2016). The angular nature of the heavy minerals in alluvia is a conserved primary relict feature during weathering and transportation. These angular grains may probably be a product of short hydromechanical transportation (Kanouo et al. 2012). In addition, the geomorphology and the tropical humid climate of the region are favorable for the deposition of alluvial placers currently mined for gold and diamonds. Therefore, we suggest that niobium-tantalum minerals from the Ngoura placers must have been sourced from the weathering and erosion of granites and pegmatites occurring in the study area (Fig. 5).

6 Conclusion

The alluvia from Ngoura are rich in niobium-tantalum oxides comprising tapiolite-(Fe) and tantalite-(Mn). Tapiolite-(Fe) plots within a narrow range of Ta* (0.900–0.933) and Mn*(0.037–0.119) typical of tapiolite-(Fe) worldwide whilst tantalite-(Mn) displays a wider range of Mn* (0.538–0.891). Both species exhibit oscillatory zoning which appears to be progressive in places. This zoning is interpreted as a primary magmatic feature resulting from magmas mixing, rapid cooling or degassing/decompression of the igneous system. The geomorphology of the eastern region combined with a tropical humid climate has played a key role in the deposition of alluvial placers. The heavy mineral fraction shows preserved primary features, suggesting a local provenance. It is therefore suggested that niobium-tantalum minerals from the Ngoura placers must have been sourced from the weathering and erosion of alkaline granites and pegmatites outcropping in the study area.

Acknowledgements We thank the University of Laval for electron microprobe analyses of niobium-tantalum minerals.

Compliance with ethical standards

Conflict of interest On behalf of all authors, the corresponding author states that there is no conflict of interest.

References

Alfonso P, iCordomi MC, iDraper JCM (1995) Nb-Ta-minerals from the Cap de Creus pegmatite field, eastern Pyrenees: distribution and geochemical trends. Mineral Petrol 55:53–69

Asaah AV, Zoheir B, Lehmann B, Frei D, Burgess R, Suh CE (2015) Geochemistry and geochronology of the ~ 620 Ma gold-associated Batouri granitoids, Cameroon. Int Geol Rev 57:1485–1509

Badanina EV, Sitnikova MA, Gordienko VV, Melcher F, Gäbler HE, Lodziak J, Syritso LF (2015) Mineral chemistry of columbite–tantalite from spodumene pegmatites of Kolmozero, Kola Peninsula (Russia). Ore Geol Rev 64:720–735

Bassis A, Hinderer M, Meinhold G (2016) New insights into the provenance of Saudi Arabian Palaeozoic sandstones from heavy mineral analysis and single-grain geochemistry. Sediment Geol 333:100–114

Černý P (1992) Geochemical and petrogenetic features of mineralization in rare-element granitic pegmatites in the light of current research. Appl Geochem 7:393–416

Černý P, Novak M, Chapman R (1992) Effects of sillimanite-grade metamorphism and shearing on Nb–Ta oxide minerals in granitic pegmatites: Marsikov, Northern Moravia, Czechoslovakia. Can Mineral 30:699

Fosso Tchunte P, Tchameni R, André-Mayer AS, Dakoure H, Turlin F, Poujol M, Nomo Negue E, Saha Fouotsa AN, Rouer O (2018) Evidence for Nb–Ta occurrences in the Syn-Tectonic Pan-African Mayo Salah Leucogranite (Northern Cameroon): constraints from Nb–Ta oxide mineralogy, geochemistry and U-Pb LA-ICP-MS geochronology on columbite and monazite. Minerals 8:188

Ganno S, Tsozué D, Kouankap Nono GD, Tchouatcha MS, Ngnotué T, Gamgne Takam R, Nzenti JP (2018) Geochemical constraints on the origin of banded iron formation-hosted iron ore from the archaean ntem complex (Congo Craton) in the Meyomessi Area, Southern Cameroon. Resour Geol 68:287–302

Holten T, Jamtveit B, Meakin P, Cortini M, Blundy J, Austrheim H (1997) Statistical characteristics and origin of oscillatory zoning in crystal. Am Mineral 82:596–606

Kanouo NS, Yongue-Fouateu R, Chen S, Njonfang E, Ghogomu RT, Zhao J, Sababa E (2012) Greyish-black megaclasts from the Nsanaragati gem placer, SW Cameroon: geochemical features and genesis. J Geogr Geol 4:134–146

Kanouo NS, Ekomane E, Yongue-Fouateu R, Njonfang E, Zaw K, Changqian M, Venkatesh AS (2016) Trace elements in corundum, chrysoberyl, and zircon: application to mineral exploration and provenance study of the western Mamfe gem clastic deposits (SW Cameroon, Central Africa). J Afr Earth Sci 113:35–50

Lahti SI (1987) Zoning in columbite-tantalite crystals from the granitic pegmatites of the Erajarve area, southern Finland. Geochem et Cosmochem Acta 51:509–517

Llorens González T, García Polonio F, López Moro FJ, Sanz Contreras JL, Moro Benito MC (2017) Tin-tantalum-niobium mineralization in the Penouta deposit (NW Spain): textural features and mineral chemistry to unravel the genesis and evolution of cassiterite and columbite group minerals in a peraluminous system. Ore Geol Rev 81:79–95

Mackay D, Simandl GJ (2014) Geology, market and supply chain of niobium and tantalum—a review. Miner Depos 49:1025–1047

Mackay D, Simandl GJ (2015) Niobium and tantalum: Geology, markets, and supply chains. In: Symposium on critical and strategic materials, pp 13–22

Mbanga Nyobe J, Sababa E, Bayiga EC, Ndjigui PD (2018) Mineralogical and geochemical features of alluvial sediments from the Lobo watershed (Southern Cameroon): implications for rutile exploration. C R Geosci 350:119–129

Mbih KP, Meffre S, Yongue-Fouateu R, Kanouo NS, Jay T (2016) Chemistry and origin of the Mayo Kila sapphires, NW region Cameroon (Central Africa): their possible relationship with the Cameroon volcanic line. J Afr Earth Sci 118:263–273

McClenaghan B, Peuraniemi V, Lehtonen M (2011) Indicator mineral methods in mineral exploration. Workshop in the 25th international applied geochemistry symposium 2011, 22–26 August 2011 Rovaniemi, Finland. Vuorimiesyhdistys, B92–4, p 72

Melcher F, Graupner T, Gabler HE, Sitnikova MA, Henjes-Kunst F, Oberthur T, Gerdes A, Dewaele S (2015) Tantalum–(niobium–tin) mineralisation in African pegmatites and rare metal granites: constraints from Ta–Nb oxide mineralogy, geochemistry and U-Pb geochronology. Ore Geol Rev 64:667–719

Mitchell RH (2015) Primary and secondary niobium mineral deposits associated with carbonatites. Ore Geol Rev 64:626–641

Mücke A, Neumann U (2006) Die mafischenMineralien und oxidischenErze der Alkali-Granite und benachbarterFlusssedimente des Jos Plateaus in Zentralnigeria:Petrografie, Mineralogie und Genese. Aufschluss 57:275–300

Ndong BF, Messi OJE, Ntomba MS, Akam JM, Mvondo OJ (2015) Apport des linéaments satellitaires pour la recherche des indices aurifères du massif éburnéen de Ngovayang au sud Cameroun (Craton du Congo). Int J Innov Appl Stud 13:368–376

Ndong BF, Sobdjou KC, Mero Y, Ntomba MS, Nzenti JP, Mvondo OJ (2016) Origin and tectonic framework of the ngovayang iron Massifs, South Cameroon. Sci Res 4:11–20

Nguimatsa DFW, Yongue-Fouateu R, Bolarinwa AT, Ngatcha RB, Fuanya C, Kamga MA (2019a) Contribution to the study of bauxites' formation in the Fongo-Tongo (Western Cameroon) sites. In: Doronzo D, Schingaro E, Armstrong-Altrin J, Zoheir B (eds) Petrogenesis and exploration of the earth's interior. Springer, Cham, pp 241–244

Nguimatsa DFW, Chapman RJ, Bolarinwa AT, Yongue-Fouateu R, Banks DA, Olajide-Kayode JO (2019b) Microchemical characterization of placer gold grains from the Meyos-Essabikoula area, Ntem complex, southern Cameroon. J Afr Earth Sci 151:189–201

Njiosseu ELT, Nzenti JP, Njanko T, Kapajika B, Nédélec A (2005) New UPb zircon ages from Tonga (Cameroon): coexisting Eburnean-Transamazonian (2.1 Ga) and Pan-African (0.6 Ga) imprints. C R Geosci 337:551–562

Nowak I, Ziolek M (1999) Niobium compounds: preparation, characterization, and application in heterogeneous catalysis. Chem Rev 99:3603–3624

Ntep Gweth P, Dupuy JJ, Matip O, Fombutu AF, Kalngui E (2003) Mineral resources of Cameroon. Sopecam, Yaoundé, p 417

Simandl GJ, Burr RO, Trueman DL, Paradis S (2018) Economic geology models 2. Tantalum and niobium: deposits, resources, exploration methods and market—a primer for geoscientists. Geosci Can 45:85–96

Soh Tamehe L, Chongtao W, Ganno S, Simon SJ, Kouankap Nono GD, Nzenti JP, Lin NH (2019) Geology of the Gouap iron deposit, Congo craton, ta southern Cameroon: implications for iron ore exploration. Ore Geol Rev 107:1097–1128

Suh CE, Lehmann B, Mafany GT (2006) Geology and geochemical aspects of lode gold mineralization at Dimako-Mboscorro, SE Cameroon. Geochem Explor Environ Anal 6:295–309

Takodjou Wambo JD, Ganno S, Ngambu AA, Nomo Negue E, Ondoa JM, Nzenti JP (2016) Use of landsat 7 ETM + Data for the geological structure interpretation: case study of the Ngoura-Colomines Area, Eastern Cameroon. J Geosci Geomat 4:61–72

Takodjou Wambo JD, Ganno S, Lahe YSD, Kouankap Nono GD, Fossi DH, Tchouatcha MS, Nzenti JP (2018) Geostatistical and GIS analysis of the spatial variability of alluvial gold content in Ngoura-Colomines area, Eastern Cameroon: implications for the exploration of primary gold deposit. J Afr Earth Sci 142:138–157

Teutsong T, Bontognali TRR, Ndjigui PD, Vrijmoed JC, Teagle D, Cooper M, Vance D (2017) Petrography and geochemistry of the Mesoarchean Bikoula banded iron formation in the Ntem complex (Congo craton), Southern Cameroon: implications for its origin. Ore Geol Rev 80:267–288

Tindle AG, Breaks FW (2000) Columbite-tantalite mineral chemistry from rare-element granitic pegmatites: separation Lakeh area, NW Ontario, Canada. Mineral Petrol 70:165–198

Tonje JC, Ndjigui PD, Nyeck B, Bilong P (2014) Geochemical features of the Matomb alluvial rutile from the Neoproterozoic Pan-African belt, Southern Cameroon. Chemie der Erde-Geochem 74:557–570

Toteu SF, Penaye J, Djomani YP (2004) Geodynamic evolution of the Pan-African belt in central Africa with special reference to Cameroon. Can J Earth Sci 41:73–85

Van Lichtervelde M, Salvi S, Beziat D, Linnen R (2007) Textural features and chemical evolution in tantalum oxides: magmatic versus hydrothermal origins for Ta mineralization in the Tanco Lower pegmatite, Manitoba Canada. Econ Geol 102:257–276

Van Schmus WR, Oliveira EP, Da Silva Filho AF, Toteu SF, Penaye J, Guimarães IP (2008) Proterozoic links between the Borborema province, NE Brazil, and the central African fold belt. Geol Soc Lond Spec Publ 294:69–99
Vishiti A, Suh CE, Lehmann B, Egbe JA, Shemang EM (2015) Gold grade variation and particle microchemistry in exploration pits of the Batouri gold district, SE Cameroon. J Afr Earth Sci 111:1–13
Wise MA, Černý P (1996) The crystal chemistry of the tapiolite series. Can Mineral 34:631–647